Electronic Supplementary Material (ESI) for Journal of Materials Chemistry A.
This journal is © The Royal Society of Chemistry 2019

Supporting Information for

Plasma-activated CoO_x nanocluster supported on graphite intercalation compounds for improved CO_2 electroreduction to formate

Qiang Zhang, Anbang He, Yong Yang, Jun Du*, Zouhua Liu and Changyuan Tao*

College of Chemistry and Chemical Engineering, Chongqing University, Chongqing 400044, China.

**Corresponding authors: College of Chemistry and Chemical Engineering, Chongqing University, Chongqing 401331, China.*
E-mail addresses: dujune@cqu.edu.cn (Jun Du), taocy@cqu.edu.cn (Changyuan Tao).

Mailing address for correspondence:

Dr. Du, Jun (Prof.)

College of Chemistry and Chemical Engineering, Chongqing University

No.55 Daxuecheng South Rd., Shapingba

Chongqing 401331, China

Tel: +86-23-625678923

Fax: +86-23-625678923

E-mail: dujune@cqu.edu.cn

Electrochemical Measurements

In all measurements, we used SCE as the reference electrode. For comparison with the literature, all the potentials in this paper were converted to the RHE reference:

$$E(vs.\ RHE) = E(vs.SCE)+0.24\ V+0.059*pH$$

CO_2ER was conducted in CO_2-saturated 0.1 M $KHCO_3$ solution (pH 6.8) at room temperature and atmospheric pressure.

Calculation for Activity Descriptors

Faradaic efficiency (FE) of gaseous products at each applied potential was calculated based on the equation:

$$FE = \frac{z \cdot P \cdot F \cdot V \cdot v_i}{R \cdot T \cdot J}$$

Partial current density for formate normalized by the geometrical electrode area (J_{formate}, A cm^{-2}) was determined by calculating the total current density multiplied by FE of formate:

$$J_{formate} = FE_{formate} \cdot J$$

Formate mass activity was determined by formate partial current density divided by catalyst mass on the electrode:

$$Mass\ activity = \frac{J_{formate}}{m}$$

Formate production rate normalized by the geometrical electrode area (n, $mol \cdot cm^{-2} \cdot h^{-1}$) was calculated based on the formula:

$$n = \frac{P \cdot V \cdot v_i}{R \cdot T} \times 3600$$

Turnover Frequency (TOF, h^{-1}) for formate production per metal site is defined as the mole of formate product formed divided by the mole of Co metals in catalysts employed in the CO_2 electrolysis per hour, which can be obtained by following formula:

$$TOF = \frac{n \cdot M}{m \cdot \omega}$$

Where z is the number of electrons transferred per mole of gas product (z is 4 for formate), F is Faraday constant (96500 $C \cdot mol^{-1}$), P is pressure (1.01×10^5 Pa), V is the gas volumetric flow rate (3.33×10^{-7} $m^3 \cdot s^{-1}$), v_i is the volume concentration of gas product determined by GC, T is the temperature (298.15 K), R is the gas constant (8.314 J $mol^{-1} \cdot K^{-1}$), J is the steady-state current at each applied potential (A), m is the catalyst mass on the electrode ($g \cdot cm^{-2}$), ω is the mass percentage of Co metal in the catalysts detected by EDS, and M is atomic mass of metal ($g \cdot mol^{-1}$).

To evaluate the effect of surface area, we measured the electrochemically active surface area (ECSA) for different catalysts electrodes from the electrochemical double-layer capacitance of the catalytic surface [1]. The electrochemical capacitance was determined by measuring the non-Faradaic capacitive current associated with double-layer charging from the scan-rate dependence of cyclic voltammograms (CVs). The double-layer charging current is equal to the product of the scan rate, v, and the electrochemical double-layer capacitance, C_{DL}, as given by the equation:

$$i_c = vC_{DL}$$

Thus, a plot of i_c as a function of v yields a straight line with a slope equal to C_{DL}. The

specific ECSA of the electrodes is calculated from the double layer capacitance according to the equation:

$$ECSA=C_{DL}/C_s$$

Where C_s is the specific capacitance of the sample or the capacitance of an atomically smooth planar surface of the material per unit area under identical electrolyte conditions. For our estimates of surface area, we use general specific capacitances of Cs = 0.020 mF based on typical reported values [1].

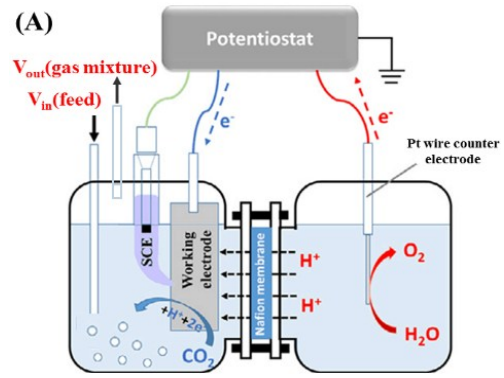

Fig. S1 schematic diagram of the electrolytic cell configuration for the electroreduction of CO_2 supplied directly from the gas phase.

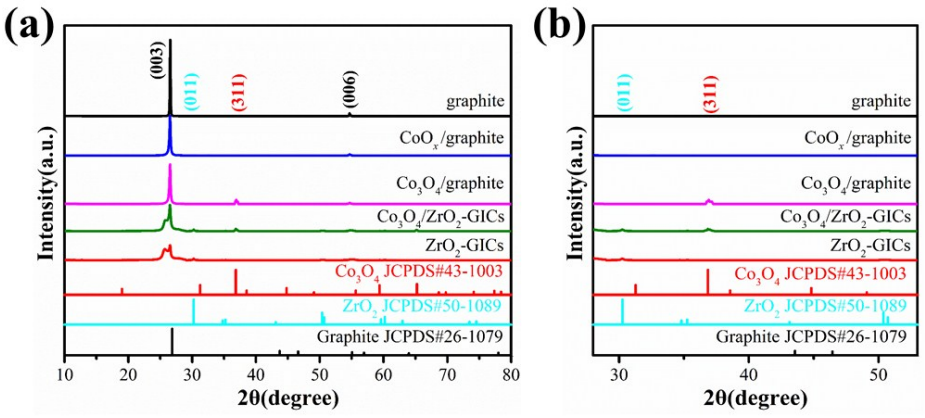

Fig. S2 (a) XRD patterns (10~90°) of graphite, ZrO_2-GICs, Co_3O_4/graphite, CoO_x/graphite and Co_3O_4/ZrO_2-GICs; (b) XRD patterns (28~53°) of graphite, ZrO_2-GICs, Co_3O_4/graphite, CoO_x/graphite and Co_3O_4/ZrO_2-GICs.

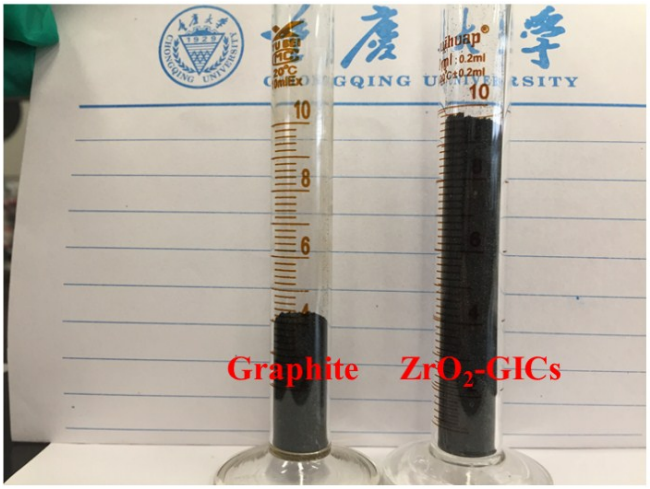

Fig. S3 The volume of graphite and ZrO_2-GICs with the same quality (0.1 g).

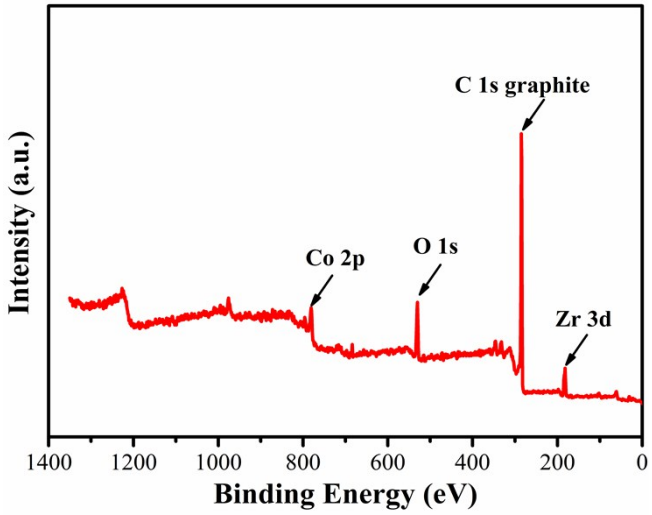

Fig. S4 XPS survey scan of CoO_x/ZrO_2-GICs.

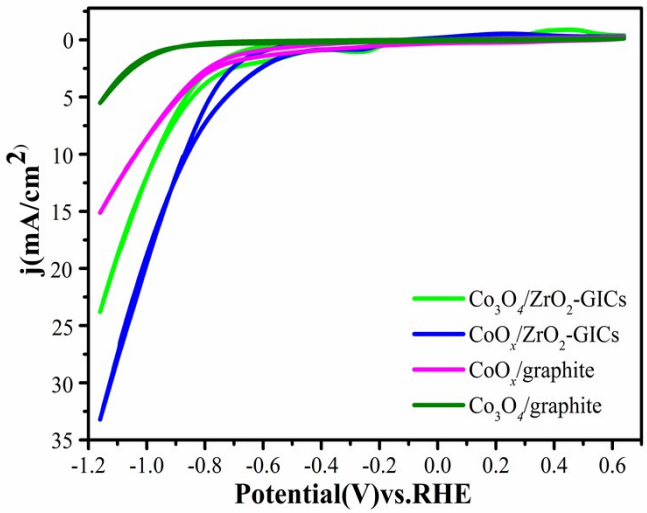

Fig. S5 CV scans of Co_3O_4/graphite, CoO_x/graphite, Co_3O_4/ZrO_2-GICs and CoO_x/ZrO_2-GICs with CO_2 in 0.1 M $KHCO_3$.

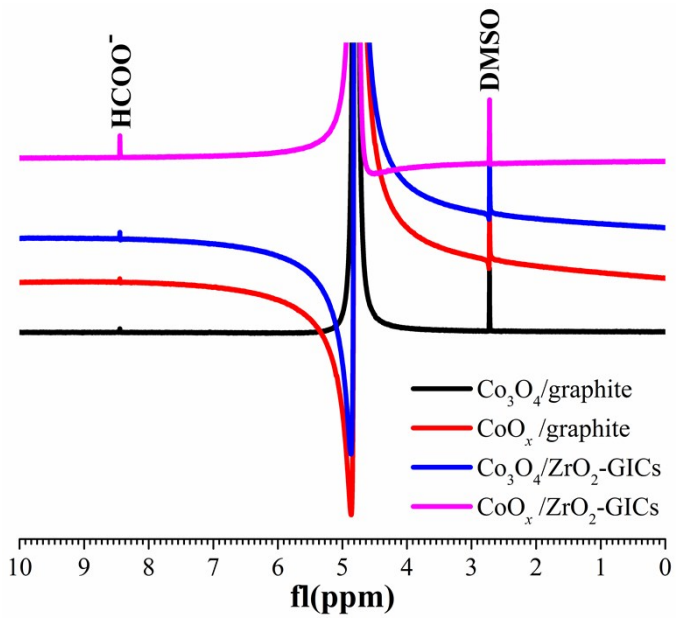

Fig. S6 ^{1}H-NMR spectra of the liquid products of CO_2RR on different catalysts at -0.85 V vs. RHE for 5h.

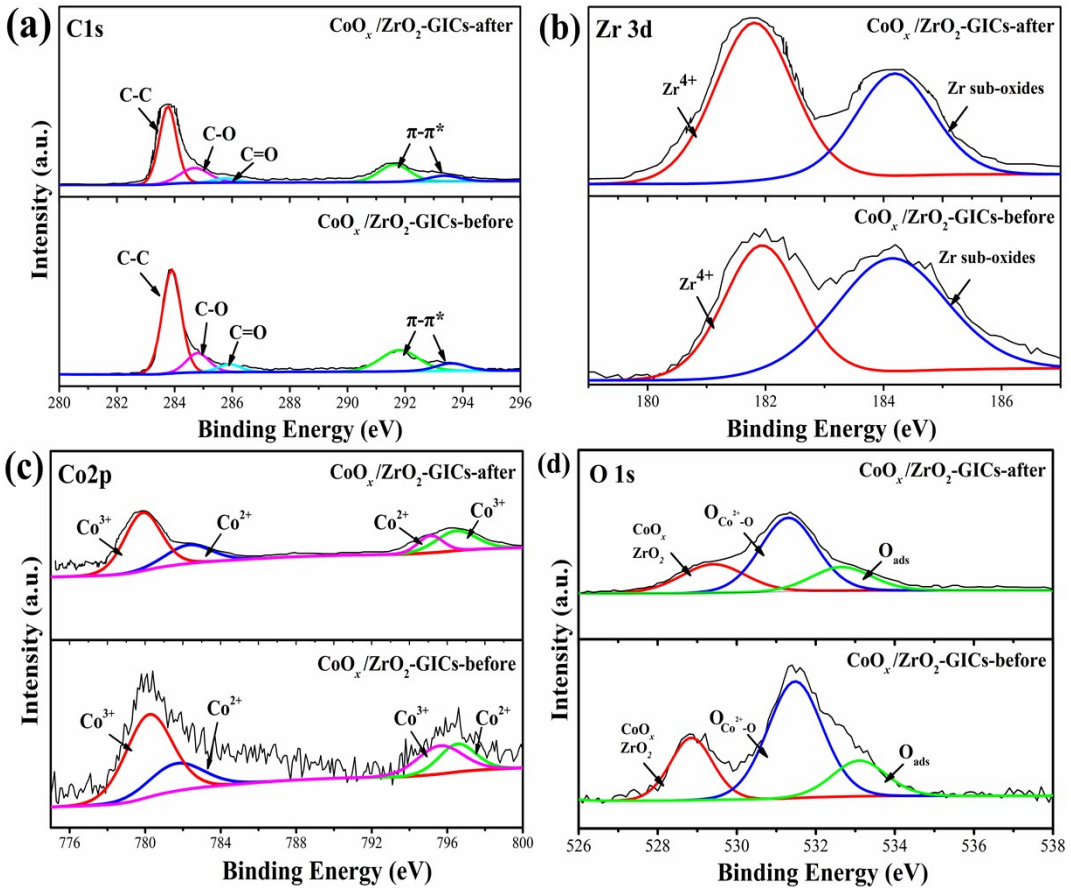

Fig. S7 XPS spectrum of CoO_x /ZrO_2-GICs before and after applied potential (-0.85 V *vs.* RHE, continuous electrolysis for 2 h) : (a) C 1s, (b) Zr 3d, (c) Co 2p, (d) O 1s.

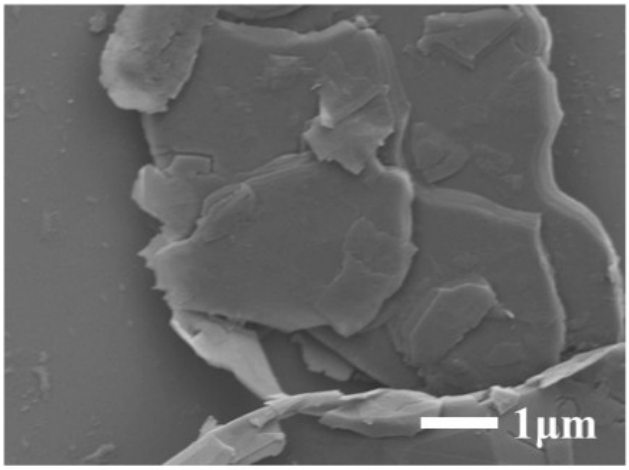

Fig. S8 SEM image of graphite-C.

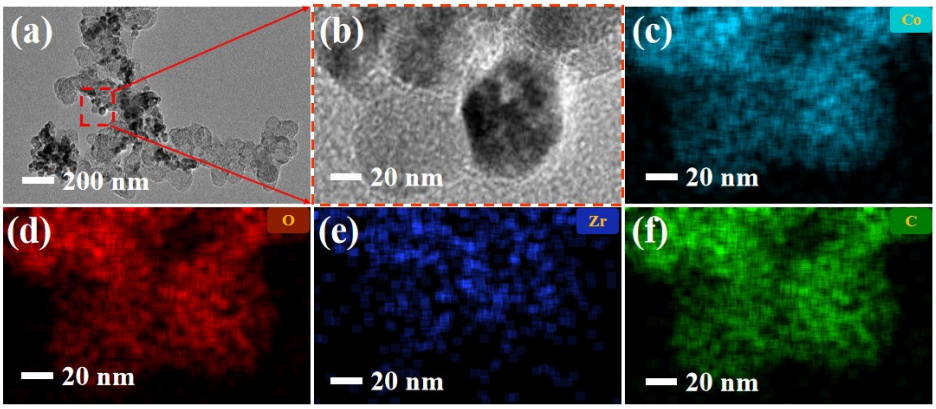

Fig. S9 TEM images of CoO_x/ZrO_2-GICs. Element distribution mapping for (c) Co, (d) O, (j) Zr, (k) C of CoO_x/ZrO_2-GICs.

Table S1 Surface elemental composition and chemical state of different catalysts as probed by XPS.

Catalyst	Co 2p (%)			O 1s (%)		
	Co^{2+}	Co^{3+}	Co^{2+}/Co^{3+}	$O_{latt}+O_{low\text{-}defect}$	O_{ads}	$(O_{latt}+O_{low\text{-}defect})/O_{ads}$
Co_3O_4/graphite	32.43	67.57	0.48	90.78	9.22	9.85
CoO_x/graphite	40.12	59.88	0.67	87.75	12.25	7.16
Co_3O_4/ZrO_2-GICs	33.77	66.23	0.51	91.95	8.05	11.43
CoO_x/ZrO_2-GIC	40.83	59.17	0.69	90.67	9.33	9.71

Table S2 Co^{2+}:Co^{3+} ratio of CoO_x/ZrO_2-GIC before and after applied potential (-0.35 V *vs.* RHE, continuous electrolysis for 2 h).

Catalyst	Co 2p (%)		
	Co^{2+}	Co^{3+}	Co^{2+}/Co^{3+}
CoO_x/ZrO_2-GIC -before	40.8	59.2	0.69
CoO_x/ZrO_2-GIC-after	41.5	58.5	0.71

Table S3 The composition quantification of different catalysts analyzed by ICP.

Catalyst	Zr(wt.%)	Co(wt.%)	O(wt.%)	C(wt.%)
Co_3O_4/graphite	0	3.0	3.6	93.4
CoO_x/graphite	0	2.9	3.1	94.0
Co_3O_4/ZrO_2-GICs	10.2	2.9	4.9	82..0
CoO_x/ZrO_2-GICs	9.6	2.8	4.0	83.6

Table S4 Electrochemical CO_2RR properties of Co-base electrocatalysts compared with other metal materials for formate production.

	Catalysts	Electrolyte	Work potential	Formate faradaic efficiency	Stability	Ref.
Other metal catalysts	Cu@Sn	0.1 M $KHCO_3$	-1.1 V vs. RHE	90.4%	10 h	18
	Bi nanoflakes	0.1 M $KHCO_3$	-0.6 V vs. RHE	100%	10 h	19
	nano-Bi	0.5 M $KHCO_3$	-1.6 V vs. SCE	98.4%	14 h	20
	SnO*x*/AgO*x*	0.1 M $KHCO_3$	-0.8 V vs. RHE	~30%	20 h	21
	Bi /Bi_2O_3	0.5 M $KHCO_3$	-0.86 V vs. RHE	100%	~24 h	22
	Sn-Bi	0.1 M $KHCO_3$	-1.1 V vs. RHE	96%	100 h	23
	sub-2 nm SnO_2 Quantum Wires	0.1 M $KHCO_3$	-0.956 V vs. RHE	74.04%	7 h	24
	Bi_2O_3NSs@MCCM	0.1 M $KHCO_3$	-0.956 V vs. RHE	73.6%	12 h	25
	Mo@NG-2	saturated KCl solution	-1.4 V vs. RHE	29%	~76 h	26
Co-based catalysts	Ultrathin Co_3O_4 layers	0.1 M $KHCO_3$	-0.24 V vs. RHE	60%	20 h	16
	V_o-rich Co_3O_4	0.1 M $KHCO_3$	-0.23 V vs. RHE	85%	40 h	17
	Co_3O_4 nanofibers	0.1M $TBAPF_6$ in CAN + 1%vol H_2O	-1.5 V vs. NHE	27%	8 h	27
	Molecular Co complexes	0.5 M $KHCO_3$	-2 V vs. $Fc^{+/0}$	90%	~1 h	28
	Cobalt protoporphyrin	0.1 M $HClO_4$	-0.6 V vs. RHE	N.A.	1 h	29
	Atomic Cobalt layers	0.1 M Na_2SO_4	-0.85 V vs. SCE	90%	60 h	30
	Co_3O_4 nitrogen doped graphene	0.1 M $KHCO_3$	-0.95 V vs. SCE	83%	8 h	31
	Cu-Co nanoparticles	0.1 M $KHCO_3$	-1.1 V vs. RHE	10%	N.A.	32
	Co complex	0.1 M $n$$Bu_4NPF_6$/$CH_3CN$	-1.05 V vs. NHE	80%	~9 h	33
	CoO_x/ZrO_2-GICs	0.1 M $KHCO_3$	-0.35 V vs. RHE	98.4%	60 h	This work

References

[1] G. Passard, A.M. Ullman, C.N. Brodsky, D.G. Nocera, J. Am. Chem. Soc. 138 (2016) 2925-2928.